Long surface wave dynamics along a convex bottom

Ira Didenkulova,[1] Efim Pelinovsky,[2,3] and Tarmo Soomere[1]

[1]   Long linear wave transformation in a basin of varying depth is studied for a case of a convex bottom profile $h(x) \sim x^{4/3}$. This bottom geometry provides the "nonreflecting" wave propagation at least in the framework of the one-dimensional shallow water equation. In this case, shoaling effects are very strong and wave reflection occurs in the immediate vicinity of the shoreline. The existence of traveling wave solutions (which propagate without reflection) in this geometry is established through construction of a 1:1 transformation of the general 1-D wave equation to the analogous wave equation with constant coefficients. The general solution of the Cauchy problem consists of two traveling waves propagating in opposite directions and allows a detailed description of the wavefield (vertical displacement and depth-averaged flow). It is found that generally a zone of weak current is formed between these two waves. Waves are reflected from the coastline so that their profile is inverted with respect to the calm water surface. Long-wave runup on a beach with this profile is studied for the sine pulse, Korteweg-de Vries soliton, and N wave. It is shown that in certain cases the runup height along the convex profile is considerably larger than for beaches with a linear slope. The analysis of wave reflection from the border of a shallow coastal area of constant depth and a section with the convex profile shows that a transmitted wave always has a sign-variable shape. Results of the wave transformation above the convex beach and beaches following a general power law are compared. This simplified model demonstrates the potential importance of the tsunami wave transformation along convex beaches.

1.   Introduction

[2]   The wave transformation and shoaling of water waves in basins of variable depth is a well developed task of fluid dynamics and has numerous applications in physical oceanography [*Le Blond and Mysak*, 1978; *Mei*, 1989; *Massel*, 1989; *Dingemans*, 1996]. Asymptotic methods are widely applied to describe the wavefield for slow variations of the water depth [*Shen*, 1975; *Mei*, 1989; *Dingemans*, 1996; *Berry*, 2005; *Dobrokhotov et al.*, 2006, 2007]. In the simplified case of 1-D linear shallow water wave propagation, asymptotic methods lead to the well-known Green's law, $A \sim h^{-1/4}$, for the change in the wave amplitude A (h is a water depth), derived from the energy flux conservation. Not all amplitude changes follow this law; for example, the height of a solitary wave (soliton) may vary as $A \sim h^{-1}$ in the framework of the weakly nonlinear theory of dispersive waves [*Grimshaw*, 1970; *Ostrovsky and Pelinovsky*, 1970]. A more complicated formula can be obtained for the solitary

wave of an arbitrary height [*Pelinovsky*, 1996]. The particular law of dependence of the wave amplitude on the combination of the properties of the attacking wave and of the medium, and the related problem of wave runup, is one of the central questions in modeling of tsunamis and coastal flooding.

[3]   If the water depth in the coastal zone is rapidly varying, the exact analytical solutions for wave transformation can be found within linear shallow water theory for different bottom profiles. Such solutions usually are expressed in terms of special functions [*Le Blond and Mysak*, 1978; *Massel*, 1989; *Mei*, 1989]. Analytical, rigorous solutions of the nonlinear shallow water system are only known to exist for beaches of constant slope [*Carrier and Greenspan*, 1958]. The solution of the nonlinear problem strongly depends on the initial waveshape. Various shapes of the periodic incident wave trains such as the sine wave [*Kaistrenko et al.*, 1991; *Madsen and Fuhrman*, 2007], cnoidal wave [*Synolakis*, 1991] and nonlinear deformed periodic waves [*Didenkulova et al.*, 2006, 2007] have been analyzed in the literature. The relevant analysis has been also performed for a variety of solitary waves and single pulses such as soliton [*Pedersen and Gjevik*, 1983; *Synolakis*, 1987; *Kânoğlu*, 2004], sine pulse [*Mazova et al.*, 1991; *Didenkulova and Pelinovsky*, 2008], Lorentz pulse [*Pelinovsky and Mazova*, 1992], Gaussian pulse [*Carrier et al.*, 2003; *Kânoğlu and Synolakis*, 2006], N waves [*Tadepalli*

---

[1]Institute of Cybernetics, Tallinn University of Technology, Tallinn, Estonia.
[2]Department of Nonlinear Geophysical Processes, Institute of Applied Physics, Russian Academy of Sciences, Nizhny Novgorod, Russia.
[3]Department of Mathematical Sciences, Loughborough University, Loughborough, UK.
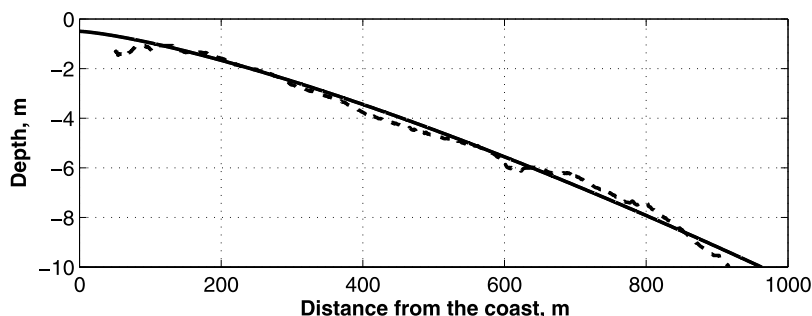
Figure 1. Measured bottom profile at Pirita Beach, Estonia (dashed line) and its power asymptotic (solid line).

and *Synolakis*, 1994], and "characterized tsunami waves" [*Tinti and Tonini*, 2005]. The numerical methods are now widely applied to study wave transformation and shoaling in the coastal zone (see review paper by *Dalrymple et al.* [2006]).

[4] The approximation of a linearly varying depth is not particularly realistic. Various equilibrium bottom profiles in the vicinity of the shoreline including power asymptotic $h(x) \sim x^d$ are discussed in literature. The most common is the famous Dean's Equilibrium Profile with $d = 2/3$ [see, e.g., *Dean and Dalrymple*, 2002]. For Dutch dunes profiles $d = 0.78$ provides a better fit [*Steetzel*, 1993]. *Kit and Pelinovsky* [1998] found a range of $d = 0.73 - 1.1$ for Israeli beaches. Various asymptotic approximations for beach profiles in terms of power laws are also used in theoretical models [*Kobayashi*, 1987; *Kit and Pelinovsky*, 1998]. However, in many cases, bottom profiles have a composite structure with one shape near the beach and another profile shape at greater depths. Figure 1 demonstrates the bottom profile measured at Pirita Beach, Estonia [*Soomere et al.*, 2007]. It is clearly seen that the profile for the depths of $2 - 10$ m can be approximated by the power law with $d = 4/3$. A similar approximation with $d > 1$ can be found for continental Pacific shelf of Northern Chile for the coastal line down to the depth of 5 km (Figure 2).

[5] Therefore, it is important to analyze the wave transformation and runup for various realistic bottom profiles matching more general power laws (not only the popular case $d = 1$). The case $d = 4/3$ is of special interest, because the solution of linearized shallow water equations can be

obtained in elementary functions for this profile [*Cherkesov*, 1976; *Pelinovsky*, 1996; *Tinti et al.*, 2001]. In previous studies, this case was considered mainly to simplify the final expressions describing wave dynamics, but a comprehensive analysis of wave properties and transformation along this type of coastal slope is missing.

[6] In this paper we study the linear dynamics of shallow water waves for the convex depth profile $h(x) \sim x^{4/3}$ for a wide class of initial conditions. The main aim is to establish the potential threats to the coastal zone through enhanced amplitude amplification of approaching waves and potentially larger runup height of long waves along beaches containing convex sections of the coastal slope. The paper is organized as follows. The properties of traveling waves along the convex bottom are described in section 2. The uniqueness of such traveling wave solutions is proved in section 3 by means of introducing a 1:1 transformation of the governing wave equation with varying coefficients to the constant coefficient wave equation. This transformation enables us to obtain the solution of the Cauchy problem and to study wave evolution for various initial conditions in a straightforward manner. Wave runup on a beach of a special profile with $d = 4/3$ is analyzed in section 4, with an important implication that wave amplification for such a beach can be much more significant than for a plane beach. The monochromatic wavefield in the basin of a general power profile is described in section 5. Special attention is paid to the phase shift between reflected and incident waves versus a profile power. The wave propagation along the beach containing a shallow coastal area and a section of
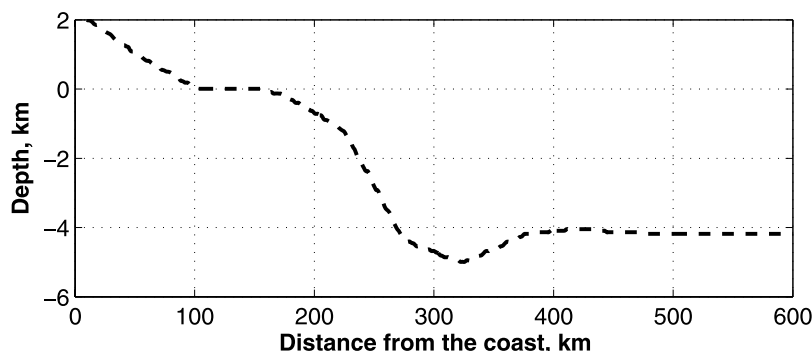
Figure 2. Bottom profile extracted from the Historical Tsunami Database [*Gusiakov*, 2002] for Pacific coast of northern Chile at 7.7°S 78.51°W.

convex beach is studied in section 6. The main results are summarized in conclusion.

2. Traveling Waves Above an Uneven Bottom

[7] The basic model for the linear, long-crested, 2-D shallow water waves in the basin of a variable depth is a 1-D linear wave equation for the vertical displacement of the water surface $\eta(x, t)$

$$\frac{\partial^2 \eta}{\partial t^2} - \frac{\partial}{\partial x}\left[c^2(x)\frac{\partial \eta}{\partial x}\right] = 0, \; c(x) = \sqrt{gh(x)}, \qquad (1)$$

where $c(x)$ is the wave speed, $h(x)$ is the water depth and g is the gravity acceleration. The domain, boundary and initial conditions for equation (1) will be discussed later.

[8] Traveling wave solutions for the wave equation with slowly varying coefficients, equivalently, for the waves above slowly varying bottom relief, are usually studied with the use of asymptotic methods. Exact solution of the wave equation for a sine wave above a convex beach with power $d = 4/3$ has the same form [Cherkesov, 1976; Pelinovsky, 1996]. We will shortly recall these results from the viewpoint of the structure of the traveling water waves.

[9] Traveling (progressive) waves are sought in the form

$$\eta(x, t) = A(x)\exp\{i[\omega t - \Psi(x)]\}, \qquad (2)$$

where $A(x)$ and $\Psi(x)$ are real functions (local amplitude and phase, respectively) which should be determined, and ω is the wave frequency. After substitution of equation (2) to equation (1) the real and imaginary parts of the resulting equation are the following two ordinary differential equations:

$$\left[\frac{\omega^2}{gh(x)} - k^2(x)\right]A + \left[\frac{d^2A}{dx^2} + \frac{1}{h}\frac{dh}{dx}\frac{dA}{dx}\right] = 0, \qquad (3)$$

$$2k\frac{dA}{dx} + A\frac{dk}{dx} + \frac{1}{h}\frac{dh}{dx}kA = 0. \qquad (4)$$

Here $k(x) = d\Psi/dx$ is a variable wave number. Equation (3) can be interpreted as the generalized dispersion relation for waves in an inhomogeneous medium whereas equation (4) has the meaning of the energy flux conservation. While equation (4) can be easily integrated

$$A^2(x)k(x)h(x) = \text{constant}, \qquad (5)$$

equation (3) is a second-order differential equation with variable coefficients which generally has no analytic solutions in closed form. This equation is not simpler than the initial wave equation (1).

[10] Further progress toward analytically solving equation (3) can be made when the wave propagates above a slowly varying bottom. In this case both variations of the water depth and the wave amplitude are slow; the terms in the second bracket of equation (3) are small compared to

other additives and can be ignored in the first approximation. In this case, equation (3) is simply solved

$$k(x) = \frac{\omega}{\sqrt{gh(x)}}. \qquad (6)$$

Equation (6) is a generalization of the well-known dispersion relation for water waves in the basin of slowly varying depth. Solution (6) together with equation (5), determine the wave amplitude (that in this case evidently follows Green's law) and phase. The relevant asymptotic procedure and all higher-order corrections of the wave amplitude and phase are described in detail by Maslov [1987, 1994], Babich and Buldyrev [1991], and Berry [2005].

[11] Basically, equation (3) can be solved numerically for an arbitrary function $h(x)$ or analytically for specific bottom profiles. As a result, solution (2) can be determined completely. Sometimes, solutions of this type are called traveling waves in an arbitrarily inhomogeneous medium (without any specific applications for water waves) and can be interpreted as a description of complicated physical processes of wave transformation and reflection in a basin of variable depth [Ginzburg, 1970; Brekhovskikh, 1980].

[12] We, however, concentrate on the analysis of the potential existence of exact traveling wave solutions to equation (1) and their propagation and reflection properties. The procedure to select the traveling wave solution from the entire set of solutions of equation (3), does not have a rigorous formulation in the literature. Historically, a subset of such solutions has been found by ensuring that the following two equations:

$$\frac{\omega^2}{gh(x)} - k^2(x) = 0 \qquad (7)$$

and

$$\left[\frac{d^2A}{dx^2} + \frac{1}{h}\frac{dh}{dx}\frac{dA}{dx}\right] = 0 \qquad (8)$$

are satisfied simultaneously. Obviously, any set of solutions $\{A, k, h\}$ to equations (7) and (8) also solves equation (3), although generally solutions to equation (3) do not solve equations (7) and (8) simultaneously. The solution of equation (7) is straightforward and given by equation (6); thus the function $k(x)$ is uniquely defined. The system of equations (5) and (8) is overdetermined for the wave amplitude. Its consistent solution can be achieved if and only if

$$h(x) = p(x + b)^{4/3}, \qquad (9)$$

where p and b are arbitrary constants. The desired solution therefore only exists for beaches having a specific convex bottom profile. As constant b can be eliminated by a shift $\tilde{x} = x - b$ of the x axis, we can assume $b = 0$ without the loss of generality. Doing so simply means that the origin $x = 0$ is located at the coastline. For the bottom profile presented by

equation (9) the components of the traveling wave in ansatz (2) are then completely and uniquely defined

$$k(x) = \frac{\omega}{\sqrt{gp}} x^{-2/3}, \Psi(x) = \frac{3\omega}{\sqrt{gp}} x^{1/3} + \text{const}, A(x) = \frac{\text{const}}{x^{1/3}}.$$

(10)

The corresponding full solution to equation (1) can be rewritten in traveling wave form

$$\eta(x, t) = A(x) \exp\{i\omega[t - \tau(x)]\}, A(x) = A_0 \left[\frac{h_0}{h(x)}\right]^{1/4},$$

$$\tau(x) = \int\limits_{x_0}^{x} \frac{dy}{c(y)},$$

(11)

where A_0 and h_0 are the amplitude and the water depth at the point $x = x_0$, respectively. The location of the point $x = x_0$ can be chosen arbitrarily. This feature enables analysis of waves approaching from offshore as well as waves generated in the vicinity of the coast. The solutions given by equation (11) correspond to right-going (propagating offshore in this geometry) monochromatic wave trains [*Cherkesov*, 1976; *Pelinovsky*, 1996]. The resulting expressions coincide with the asymptotic wave solution for a slowly varying bottom profile, but are correct for any bottom slope. A similar solution can be obtained for a wave propagating to the left (onshore) direction by simply picking up another sign of $\tau(x)$ in equation (11). In the linear framework the principle of linear superposition holds and these waves do not interact with each other. The resulting surface displacement or the local current in areas where they overlap is just the sum of displacements or currents caused by the counterparts.

[13] The previous studies into the problem in question have been limited to the analysis of properties of monochromatic or sine waves. An obvious generalization of the existing results is with the use of Fourier analysis to obtain the superposition of such sine waves with different frequencies, the technique obviously being applicable in this linear framework. With the use of the Fourier integral of spectral components (11), the traveling wave of an arbitrary shape can be presented in a general form

$$\eta(x, t) = A(x) f[t - \tau(x)],$$

(12)

where $f(t)$ describes the waveshape (interpreted here as the variation with time of the surface elevation at a fixed point). An important feature is that representation (12) allows consideration of wave pulses of finite duration being generalized solutions of the wave equation.

[14] Another important property of the shallow water wavefield is the wave-induced, depth-averaged flow velocity. This velocity can be calculated from the water displacement using one of the equations of the linear shallow water system

$$\frac{\partial u}{\partial t} + g \frac{\partial \eta}{\partial x} = 0.$$

(13)

In particular, the velocities induced by the monochromatic wave (11) and by a pulse (12) are

$$u(x, t) = U(x) \left[1 + \frac{\sqrt{gh}}{4hi\omega} \frac{dh}{dx}\right] \exp\{i\omega[t - \tau(x)]\},$$

$$U(x) = A(x) \sqrt{\frac{g}{h(x)}} = A_0 \sqrt{\frac{g}{h}} \left[\frac{h_0}{h(x)}\right]^{1/4},$$

(14)

$$u(x, t) = U(x) \left\{f(\xi) + \frac{\sqrt{gh}}{4h} \frac{dh}{dx} \Phi(\xi)\right\},$$

(15)

where $\Phi(\xi) = \int f(\xi)\, d\xi$ and $\xi = t - \tau(x)$. Notice that the first terms in equations (14) and (15) correspond to the asymptotic solution of equation (1) above a slowly varying bottom, for which the shapes of the water displacement and the wave-induced water flow coincide. The second term becomes important in the vicinity of the shoreline.

[15] If the wave generated at the depth h_0 is periodic (regular or irregular), there is no limitation on the waveshape. The natural restriction of realistic pulses – that the wave disturbance should have a limited energy (equivalently, finite effective wave duration) – leads to the following condition of zero setup

$$\int\limits_{-\infty}^{+\infty} f(t)\, dt = 0,$$

(16)

from which it follows that the shape of a water displacement should be sign variable. This condition, as it will be shown later, is valid for the traveling wave only. As it is not obvious from the viewpoint of the classical d'Alembert solution of the generic wave equation (which may consist of two sign-constant impulses propagating in different directions), we will discuss it in more detail in section 3 where the Cauchy problem will be solved.

3. Transformation to a Wave Equation With Constant Coefficients

[16] From the form of equation (11) it follows that the function $f[\tau(x) \pm t]$ should satisfy a wave equation with constant coefficients. The key component of the analysis of the existence and uniqueness of solutions to equation (1) corresponding to traveling waves in a basin of a variable depth is establishing a 1:1 transformation of equation (1) to a similar equation with $c(x) = \text{const}$.

[17] Let us seek the solution of equation (1) in the form

$$\eta(x, t) = B(x) H[\tau(x), t],$$

(17)

where $B(x)$ and $\tau(x)$ should be determined, and the function H satisfies the constant coefficient wave equation with $c = 1$ [see also *Tinti et al.*, 2001]

$$\frac{\partial^2 H}{\partial t^2} - \frac{\partial^2 H}{\partial \tau^2} = 0.$$

(18)

Substitution of equation (17) into equation (1) results in equation (18) if and only if the unknown functions $B(x)$ and $\tau(x)$ satisfy the following three equations:

$$\frac{d}{dx}\left[h(x)\frac{dB}{dx}\right] = 0, \qquad (19)$$

$$h(x)\frac{dB}{dx}\frac{d\tau}{dx} + \frac{d}{dx}\left[h(x)B(x)\frac{d\tau}{dx}\right] = 0, \qquad (20)$$

$$gh(x)\left(\frac{d\tau}{dx}\right)^2 = 1. \qquad (21)$$

These equations are generalizations of equations (5), (7), and (8). They are also overdetermined in the sense that they have a solution if and only if $h(x)$ is given by equation (9). In other words, the desired transformation exist if and only if the bottom profile is $h(x) \sim x^{4/3}$. This solution is unique for a reasonable choice of initial or boundary conditions and coincides with that of equations (10) and (11) if $B(x) = A(x)$. Moreover, if $B(x)$ and $\tau(x)$ together with $h(x) \sim x^{4/3}$ solve equations (19)–(21), then the transformation given by equation (18) reduces equation (1) to equation (18) for the unknown function H.

[18] The transformation (17) for the bottom profile $h(x) \sim x^{4/3}$ proves the existence of exact traveling wave solutions above strongly varying bottom relief. There is another important consequence of the existence of transformation (17): wave equation (18) has been extensively studied in mathematical physics, and many theorems and approaches can be directly applied to the particular solutions in question. In what follows, we use this connection for constructing the general solution of equation (1).

[19] Wave equation (1) has a clear meaning in the given geometry and should be solved on semiaxis ($0 < \tau < \infty$) only where the origin $x = 0$ is a singularity point of the solution. An important simplification of the problem is that the point $\tau = 0$ corresponding to the shoreline ($x = 0$) is not singular in equation (18).

[20] A realistic interpretation of the convex bottom profile in the vicinity of the point $x = 0$ is a reef crest just touching the free surface. In reality, a large part of the wave would break and/or overwash such a reef (in the linear theory, however, this phenomenon is not considered) whereas a part of the wave energy would be reflected back to the sea. As it is suggested by *Stoker* [1957] and *Sretensky* [1977] wave breaking in framework of the linear theory can be parameterized by the fully nonreflecting boundary condition. Mathematically it implies unboundedness of certain parameters of the wavefield at the point $x = 0$. According to equation (17) the wavefield is unbounded if the function H is nonzero at this point.

[21] If at the point $x = 0$ the convex profile ends with a vertical wall, the wave energy should be fully or partially reflected. Mathematically the full reflection can be described within the linear theory with the use of the following boundary condition

$$H(\tau = 0, t) = 0. \qquad (22)$$

In this case the water displacement $\eta(x = 0, t)$ and water discharge always remain bounded on the shoreline, but as it will be shown later, velocity field is unbounded.

[22] The possibility of defining different meaningful boundary conditions at the shoreline indicates that the situation at the coast in question accepts several mathematical treatments whereas it is not clear beforehand, which of those best describe the physics of water motion at the coastline. The universal consequence of the classical versions of boundary conditions in linear equations is that a certain property of the wavefield is unbounded. This implies that generic numerical methods, strictly speaking, may not be suitable for an adequate description of the situation in the vicinity of the coastline. They have been usually designed for nonsingular flows and may simply override more complex situations. The basic choice is between accepting unboundedness of either velocities or wave heights. Below we shall use the traditional concept, according to which the wave height should be bounded and volume discharge should be zero.

[23] In this case the domain for equation (18) can be formally extended to the whole axis ($-\infty < \tau < +\infty$). The extension is physically meaningful if the initial conditions are continued for $\tau < 0$ as $H(-\tau, 0) = -H(\tau, 0)$. This choice is frequently called the "imaginary mirror" reflection condition. In this case the wavefield has a clear physical interpretation in the domain $\tau \geq 0$ only. In fact, boundary condition (22) leads to the "antisymmetric" wave reflection off a beach, when each spectral component shifts on π. This process will be further discussed in section 5 and compared with a general case of bottom profiles following a power law.

[24] The general solution of the Cauchy problem for equation (1) describing free evolution of waves generated from the generic initial disturbance of the water surface and the velocity field

$$\eta(x, 0) = \eta_0(x), \quad u(x, 0) = u_0(x) \qquad (23)$$

can be expressed as

$$\eta(x, t) = \frac{1}{x^{1/3}}\left\{f_+[\tau(x) - t] + f_-[\tau(x) + t] - f_-[-\tau(x) + t]\right\}, \qquad (24)$$

$$u(x, t) = \sqrt{\frac{g}{p}}\frac{1}{x}[f_+(\tau - t) - f_-(\tau + t) - f_-(-\tau + t)]$$
$$- \frac{g}{3x^{4/3}}[\Phi_+(\tau - t) - \Phi_-(\tau + t) + \Phi_-(-\tau + t)], \qquad (25)$$

where functions f_+ and f_- (representing the waves propagating offshore and onshore, respectively) can be found from initial conditions (23) and $\Phi_\pm(\xi) = \int f_\pm(\xi)\, d\xi$. The condition (22) is satisfied automatically.

[25] In the theory of tsunami wave generation above an inclined bottom only the vertical displacement in the source is usually used [*Mei*, 1989; *Pelinovsky*, 1996; *Carrier et al.*, 2003; *Tinti and Tonini*, 2005; *Dutykh et al.*, 2006]. In this case

$$f_+ = f_- = f_0[\tau(x)] = 0.5x^{1/3}\eta_0(x). \qquad (26)$$

Generally, function f_0 can have an arbitrary shape determined by the initial displacement. Figure 3 displays
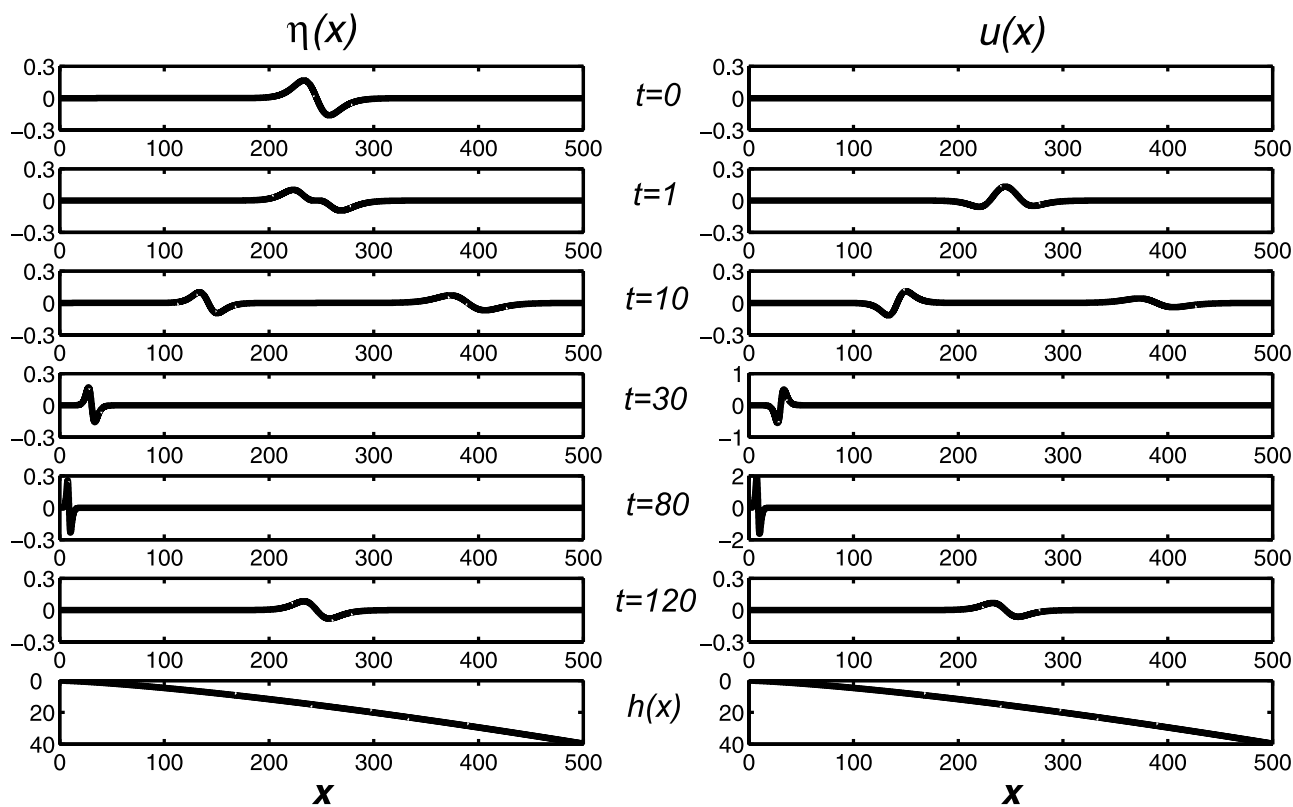
Figure 3. (left) Water displacement and (right) velocity for initial disturbance (27). The bottom profile is shown at the bottom.

the water displacement and velocity for the case, when the initial displacement in the source (located approximately at a depth of 20 m) is a sign-variable function (*N* wave, first derivative of sech^2) that satisfies equation (16)

$$f_0(\tau) = -\frac{4s}{3}\frac{\tanh[2(\tau - 60)/3]}{\cosh^2[2(\tau - 60)/3]}, \qquad (27)$$

where *s* is a numerical coefficient with dimension of m$^{4/3}$. Its particular value is unimportant in the context of this study and in the calculations below we assume that $s = 1$. The waves propagate along a convex bottom profile with a coefficient $p = 0.01$ m$^{-1/3}$, so the water depth at the distance of 500 m from the shoreline reaches 40 m.

[26] The initial disturbance is split into two waves after some time. The right-going wave moves quickly offshore. Its amplitude rapidly decreases and it propagates out of the computational domain (from 0 to 500 m) after 20 s. The amplitude of the left-going wave increases as it approaches the shore. The maximum amplitude occurs at the coastline. This scenario does not depend on the particular choice of the boundary condition on the shoreline because the wave only approaches it. In the case of the nonreflecting boundary condition, the amplitude of the wave increases to the infinity at the shoreline where it reaches within a finite time.

[27] In the case of the antisymmetric boundary condition (22) the solution experiences perfect reflection from the shore and propagates to the right with a decreasing amplitude. The two right-going waves remain separated in space.

[28] The accuracy of the calculations is estimated by means of tracking the accuracy of the conservation of the mass and energy

$$M = \int_0^\infty \eta(x,t)dx = \text{const}, \quad E = \int_0^\infty h(x)u^2(x,t)dx$$

$$+ g\int_0^\infty \eta^2(x,t)dx = \text{const} \qquad (28)$$

in our calculations $M = -0.1960$ m^2 and $E = 8.7264$ m^4/s^2. These integrals maintain their initial values with an accuracy of 10^{-8}. The kinetic and potential energies are equal after the splitting of the initial disturbance into two separated traveling waves.

[29] Another instructive example (Figure 4) is the propagation of the initial disturbance, located entirely above the calm water level. Let us consider evolution of the wave system generated from a disturbance in the form of solitary wave

$$f_0(\tau) = s\,\text{sech}^2[2(\tau - 60)/3]. \qquad (29)$$

An interesting feature here is the formation of a weak current between left-going and right-going pulses. It follows from the behavior of functions $\Phi_\pm(\xi)$ that do not vanish at both ends of the area in question. The magnitude of this current is very small, only a few percent of the maximum velocities near wave crests (Figure 5). The mass and energy
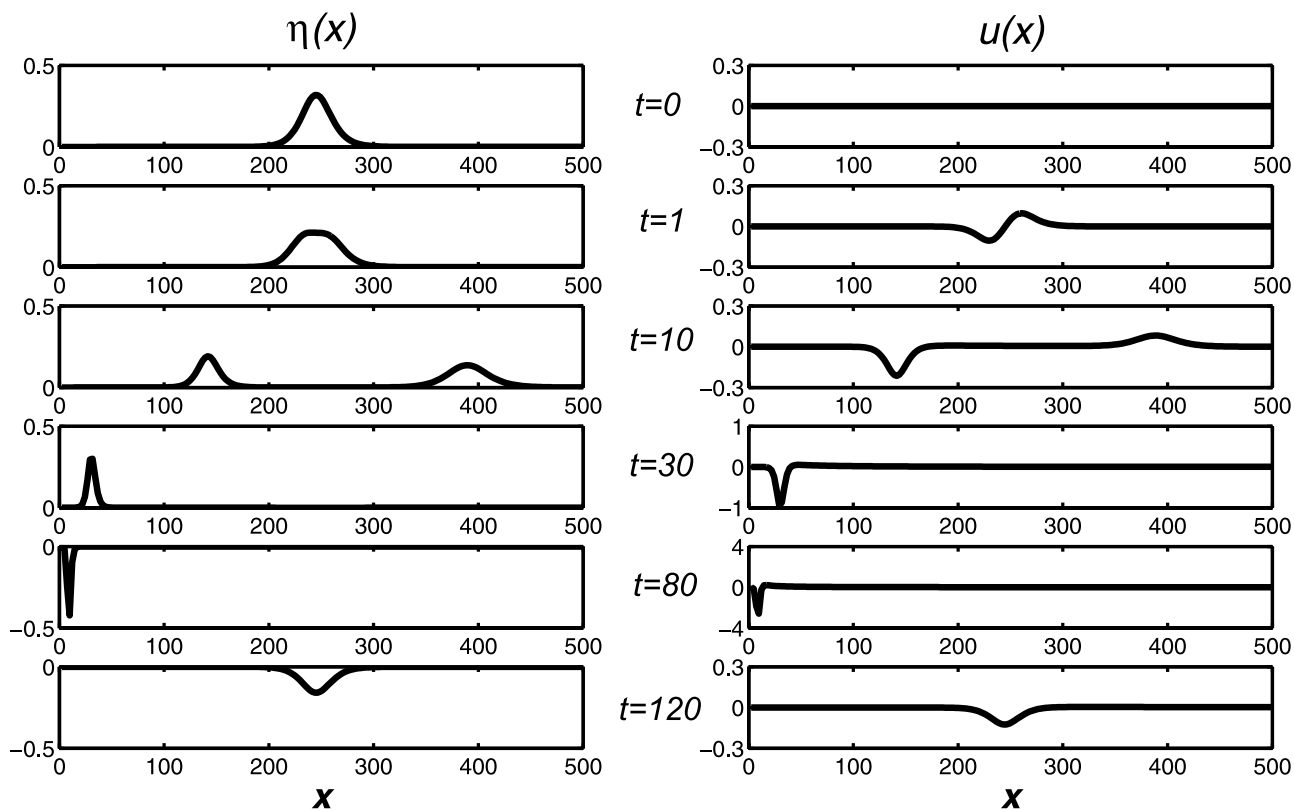
Figure 4. (left) Water displacement and (right) velocity for the initial disturbance presented by equation (29).

are also conserved here, they are equal to $M = 11.7600$ m^2 and $E = 24.5431$ m^4/s^2 with an accuracy of 10^{-8}.

[30] Initially, only positive disturbance of the water surface (elevation) is present in the system. As in the previous example, the right-going wave propagates rapidly out of the computational domain without qualitative changes in its shape. The sign of the water elevation caused by the left-going wave, however, is inverted in the process of reflection from the coastline. After this reflection, two right-going waves exist in the system, together forming a sign-variable disturbance as expected from equation (16).

[31] The appearance of the residual current is a highly interesting feature, the presence of which indicates that the wavefield contains certain other components additionally to a superposition of the traveling waves. The water velocity field evidently includes certain distributed components. The overall appearance of such a field is similar to the one that is generated during a classical wave reflection above a variable depth profile (linear or parabolic profiles) that includes the formation of a wave tail behind a shoaling pulse. The presence of such a tail can be explained for the case of the wave propagation above smoothly varying bottom profile. Conservation of the wave period and energy implies that $\lambda \sim h^{1/2}$ and $A \sim h^{-1/4}$. The water volume of the wave approaching the beach is proportional to $A\lambda \sim h^{1/4}$. Therefore, the wave must shed a part of its volume during shoaling. This local change in the water volume (which should be conserved totally) becomes evident as the current under discussion. Note that such a residual current must arise always when the shape of the disturbance is substantially deformed so that it loses (or gains) some mass. When

the entire system is mass conserving, a residual current between the sister disturbances is a natural agent that keeps the mass balance. It is eventually the strongest in the case in question when a wave of elevation is transformed into a wave of depression in the reflection process.

[32] If the depth is varying abruptly, the wave amplitude is less than the one predicted by the Green's law and the tail appears in both water elevation and velocity fields. However, in the case of the convex bottom profile the amplitude of the water elevation satisfies the Green's law and the tail appears
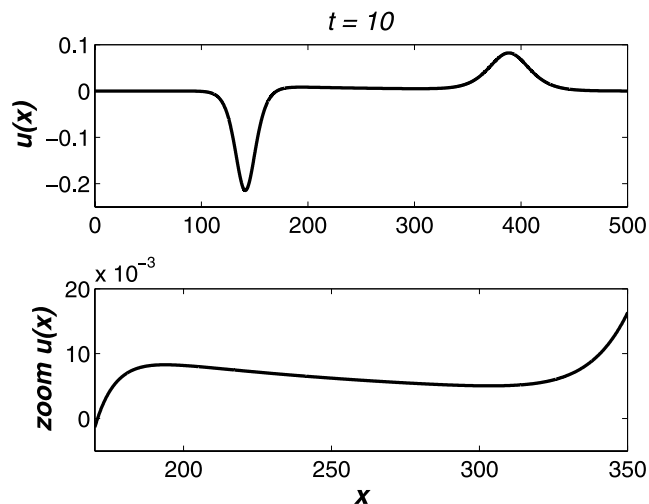
Figure 5. Formation of a space-variable current between the two pulses in Figure 4.

in the velocity field only. That is why we use inverted commas for the "nonreflecting" bottom profile: in this case the water displacement field is presented as a sum of "pure" traveling waves.

[33] It is straightforward to extend the above analysis to the case of waves propagating along an ambient current. The latter can be expressed via a nonzero initial velocity field. The procedure of finding the solution is then as follows. One of the functions, for instance f_+, can be expressed through the initial displacement (24)

$$f_+(\tau) = x^{1/3}\eta_0(x) - f_-(\tau). \qquad (30)$$

For the other function, the following differential equation for f_- (or Φ_-) can be derived from equation (25)

$$-f_-(\tau) + \frac{1}{\tau}\Phi_-(\tau) = \Upsilon(\tau), \Upsilon = \frac{h^{3/4}}{2\sqrt{g}}u_0(x) - \frac{h^{1/4}}{2}\eta_0(x)$$
$$+ \frac{1}{2\tau}\int h^{1/4}\eta_0 dx. \qquad (31)$$

This equation can be easily integrated to give

$$\Phi_-(\tau) = -\tau\int\frac{\Upsilon(\zeta)d\zeta}{\zeta}. \qquad (32)$$

The effect of the initial velocity is manifested in an additional difference between the left-going (onshore) and right-going (offshore) waves.

4. Wave Runup Along a Convex Beach

[34] From the practical point of view the behavior of the wavefield at the shoreline ($x = 0$) is the most interesting. Details of the process of wave reflection and accompanied amplitude amplification and potential runup, have important applications in tsunami modeling, forecast, and mitigation studies. Formally, linear theory is not valid in the vicinity of the shoreline where the wave amplitude becomes comparable with the water depth. In the case of a plane beach of a constant slope it has been demonstrated that the extreme runup characteristics can be calculated rigorously from linear shallow water theory even for the nonlinear problem [*Synolakis*, 1991; *Didenkulova et al.*, 2006, 2007].

[35] If the wave approaches the beach from an infinitely remote region, the wave solution of equation (1) also satisfying the boundary condition of the full reflection at the shoreline (22), has the following form [see equations (24) and (25)]:

$$\eta(x,t) = \frac{1}{x^{1/3}}\{f[t+\tau(x)] - f[t-\tau(x)]\}, \qquad (33)$$

$$u(x,t) = -\sqrt{\frac{g}{p}}\frac{1}{x}[f(t+\tau) + f(t-\tau)]$$
$$+ \frac{g}{3x^{4/3}}[\Phi(t+\tau) - \Phi(t-\tau)], \qquad (34)$$

where $f(t + \tau)$ is the shape of an incident wave approaching the shoreline $x = 0$ ($\tau = 0$). The vertical displacement of the

water surface at $x = 0$ can be found from equation (33) exactly using Taylor's series in the vicinity of $\tau = 0$

$$R(t) = \eta(0,t) = \frac{6}{\sqrt{gp}}\frac{df(t-\tau_0)}{dt}, \qquad (35)$$

where τ_0 is a travel time from a fixed point $x = L$ (chosen far offshore) to the shore. Taking into account that the incident wave at $x = L$ is

$$\eta_{in}(t) = \frac{f(t)}{L^{1/3}}, \qquad (36)$$

Equation (35) can be rewritten as

$$R(t) = 2\tau_0\frac{d\eta_{in}(t-\tau_0)}{dt}. \qquad (37)$$

Thus, the amplitude of water level oscillations at the shoreline is proportional to the vertical velocity of water particles in the incident wave. If the incident wave has the form of a solitary crest, the water level on the shoreline experiences first runup, followed by rundown. The runup height is determined by the ratio of the travel time τ_0 to the wave period T. Therefore, it is bigger if the incident wave approaches from deeper waters. This feature suggests that beaches that have extensive convex slopes offshore may experience considerable amplification of waves compared with beaches with linearly increasing depth with an amplification factor $\sqrt{\tau/T}$ [*Didenkulova et al.*, 2007]. The large shoaling above a convex bottom profile appears in the vicinity of the shoreline where a section of a small depth continues over larger distances than for a beach of constant slope. Far from the shoreline the wave amplitude follows the Green's formula for both profiles.

[36] The maximum velocity of water particles in the vicinity of the shore $x = 0$ is unbounded and proportional to

$$u(x \to 0, t) \approx -\frac{6}{p\sqrt{gp}}\frac{1}{x^{1/3}}\frac{d^2f}{dt^2}. \qquad (38)$$

This feature may be interpreted as an implicit manifestation of wave breaking. However, wave breaking is not accounted in the framework of equation (1). Although the water velocity becomes infinitely large at the shoreline, the water discharge is bounded, because

$$h(x)u(x,t) \to -\frac{6x}{\sqrt{gp}}\frac{d^2f}{dt^2} \to 0. \qquad (39)$$

The shore therefore plays a role of an equivalent to a vertical wall perfectly reflecting the wave energy from the beach.

[37] The singularity in the water velocity in the vicinity of the shoreline can be excluded by a small variation of the bottom profile, more precisely, by variations of the face slope which is zero in a given geometry. For example, in the case of a profile of a constant slope α in the vicinity of the shoreline the maximal value of water velocity on the shoreline is [*Didenkulova et al.*, 2007]

$$U_{max} = \frac{\omega\max[\eta(0,t)]}{\alpha} \qquad (40)$$
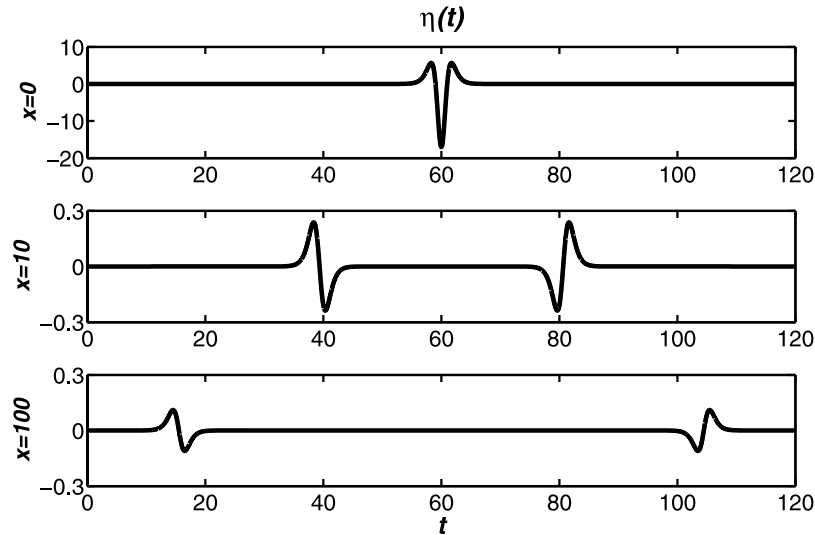
Figure 6. Time series of the water surface of the wave system generated from initial disturbance given by equation (27) at the shoreline and at two offshore points.

for a sinusoidal incident wave. This formula can be also derived from the geometry of the moving shoreline. It follows from equation (40) that the water velocity tends to the infinity when the face slope tends to zero, as for a convex bottom profile. The discharge is zero for all variations of the face slope within the linear theory.

[38] To illustrate the processes in the vicinity of the coastline, time records of the water displacement during the runup of a sign-variable wave (N wave, equation (27)), computed with the use of equation (33), are presented in Figure 6 at selected points of the coastal slope. Far from the shoreline, the time series contains both incident and reflected waves (the latter having an inverted shape as discussed above). The wave amplification when the wave approaches the shore and the transformation of the wave-shape at the shoreline are clearly seen from Figure 6. For this particular waveshape, the rundown amplitude significantly (by approximately 3 times) exceeds the runup amplitude. According to equation (37) the maximal runup height is 5.7 m, and rundown depth is 17 m for the initial amplitude of 11 cm. The wave amplitude on such a beach can be amplified by an order of magnitude and even more, if the wave breaking is neglected.

[39] As an example, let us calculate the runup height analytically for the case when the incident wave is the solitary wave solution of the Korteweg-de Vries equation

$$\eta(t) = A \mathrm{sech}^2 \left[\sqrt{\frac{3Ag}{4h^2}} t \right]. \tag{41}$$

The runup height induced by an approaching solitary wave is

$$R_{max} = 4L \left(\frac{A}{h} \right)^{3/2}. \tag{42}$$

If we introduce the mean slope of a beach $\alpha = h/L$, expression (42) can be rewritten as

$$R_{max} = 4 \frac{A}{\alpha} \sqrt{\frac{A}{h}} \sim A^{3/2}. \tag{43}$$

Comparison of this result with the asymptotic formula for runup of a solitary wave on the plane beach [*Synolakis*, 1987]

$$R_{max} = 2.8312 \frac{A}{\sqrt{\alpha}} \left(\frac{A}{h} \right)^{1/4} \sim A^{5/4}, \tag{44}$$

suggests that the runup of solitary waves of moderate amplitudes on convex beaches may lead to considerably larger inundation of the land than similar processes on beaches of constant slope.

[40] The runup of waves of an arbitrary shape can be studied in a similar way. Recently it has been shown in the framework of Carrier-Greenspan transformation for a plane beach that the runup height of asymmetric incident waves, where the face slope exceeds the back slope, is higher in comparison to the runup of symmetric waves [*Didenkulova et al.*, 2006, 2007]. This feature may be observed for beaches of various profiles and it is inherently evident from equation (37) for the convex beach.

5. Monochromatic Wavefield Over Bottom Profile Following a Power Law

[41] A convex bottom profile (9) is a particular case of a general bottom profile with a power law

$$h(x) = px^d. \tag{45}$$

The linear wave dynamics for such bottom profiles can be analyzed analytically for the particular waveshape. The

monochromatic solution of the linear wave equation (1) is expressed through the Bessel functions

$$\eta(x) = C_1 x^{\delta} J_{\nu}(\beta x^{\gamma}) + C_2 x^{\delta} N_{\nu}(\beta x^{\gamma}), \qquad (46)$$

where

$$\delta = \frac{1-d}{2}, \gamma = \frac{2-d}{2}, \nu = \frac{1-d}{2-d}, \beta = \frac{2\omega}{\sqrt{gp}(2-d)}, \qquad (47)$$

and C_1 and C_2 are arbitrary constants and we consider the case $d < 3/2$ only. The water flow is described by

$$u(x) = i\sqrt{\frac{g}{p}}x^{\delta+\gamma-1}(C_1 J_{\nu-1}(\beta x^{\gamma}) + C_2 N_{\nu-1}(\beta x^{\gamma})). \qquad (48)$$

In the case of $0 < d < 1 (1/2 > \nu > 0)$ the water displacement is bounded everywhere including the shoreline ($x = 0$). Nevertheless the water velocity is bounded on the shoreline only if $C_1 = 0$. In this case solution (46) is fully determined and represents standing wave, where C_2 can be expressed through the linear runup height R as follows:

$$\eta(x) = -R\frac{\beta^{\nu}\sin(\nu\pi)\Gamma(1-\nu)x^{\delta}}{2^{\nu}}N_{\nu}(\beta x^{\gamma}), \qquad (49)$$

where $\Gamma(\zeta)$ is the gamma function. Far from the shoreline, the wavefield is described by the asymptotic expression

$$\eta(x) = R\frac{\beta^{\nu}\sin(\nu\pi)\Gamma(1-\nu)x^{\delta}}{2^{\nu}}\sqrt{\frac{2}{\pi\beta x^{\gamma}}}\cos\left(\beta x^{\gamma} + \frac{\pi}{4} - \frac{\pi\nu}{2}\right). \qquad (50)$$

After multiplying by $\exp(i\omega t)$, the latter expression can be presented as the superposition of two waves propagating in opposite directions with the phase shift

$$\Psi = \left(\frac{1}{2} - \nu\right)\pi. \qquad (51)$$

In the case $d \to 0 (\nu \to 1/2)$, there is no phase shift between the incident and reflected waves at the shoreline. This is not unexpected, because the process is equivalent to the reflection from a vertical wall. When $d \to 1 (\nu \to 0)$, that is, in the case of a plane beach, the phase shift tends to $\pi/2$ and equation (46) becomes

$$\eta(x) = RJ_0\left(\frac{2\omega}{\sqrt{gp}}x^{1/2}\right) \qquad (52)$$

and coincides with the well-known solution presented by *Carrier and Greenspan* [1958], *Synolakis* [1987], and *Didenkulova et al.* [2007].

[42] In the case of $1 < d < 3/2 (0 > \nu > -1)$ the water displacement is bounded everywhere including the shoreline ($x = 0$) only if $C_1 = 0$. The water velocity is unbounded at the shoreline but the water discharge is still bounded as it has been demonstrated for a convex bottom profile. In this case, solution (46) coincides with equation (49) and the

phase shift is described by equation (51). The phase shift between the reflected and incident waves increases with an increase in d and reaches π for $d = 4/3$. This value of the phase shift has been obtained in section 3 in the case of a convex beach directly from the boundedness of the wavefield at the shoreline, which corresponds to the antisymmetric boundary condition (22).

[43] The wave amplification can be also studied using equation (49). Its asymptotic expression far from the shoreline coincides with the Green's law $A \sim h^{-1/4}$ for all values of d.

[44] Thus, the analysis of the wave dynamics above a power bottom profile (45) demonstrates a gradual change in the magnitude of the phase shift between the incident and reflected waves when the shape of the bottom varies from the vertical wall ($\Psi = 0$) over a constant slope ($\Psi = \pi/2$) to a convex bottom profile ($\Psi = \pi$). In the general case of a bottom profile with a power law, the wavefield cannot be split into two traveling waves (except when it is far from the shoreline where the Green's law is valid) and always contains a sort of "tail." The reason for this feature is that energy of the incident wave generally is continuously transferred into the reflected wave. This process leads to a more complicated wave dynamics than just that of two traveling waves, and, in particular, is the basic reason for emerging the residual current.

[45] Highly interesting and intriguing questions are whether reflections of this type may occur in realistic conditions and whether they can be reproduced using classical numerical methods that generally treat the sea bottom as a piecewise linear function. While almost exact representation of deeper parts of the convex nearshore by means of increasing the resolution of the models may lead to adequate results, an adequate representation of processes in the nearly singular vicinity of the shoreline may become a more demanding challenge, full solution of which may require a specific combination of analytical and numerical tools.

6. Wave Reflection From a Zone of Increasing Depth

[46] The solution obtained for a beach with a convex profile (9) contains a singularity at $x = 0$. To eliminate the role of the singularity, let us consider the situation when the water flow continues moving inland in a channel of small but finite depth. This situation is realistic at a port entrance or at a mouth of a small river with a weak current. The analysis can be done by considering the geometry of the following bottom relief in which the origin separates a shallow area of constant depth from a convex slope (Figure 7)

$$h(x) = \begin{cases} h_0 & x < 0 \\ h_0(1 + x/L)^{4/3} & x > 0 \end{cases}. \qquad (53)$$

In this case, both the velocity field and water displacement are bounded everywhere. As the coastal slope is discontinuous at the origin, the presence of this inflection point gives rise to a specific problem of transmission of wave energy between different areas and reflection from this point.

[47] Let us first consider the case when an incident sine wave approaches the convex coast from a zone of constant
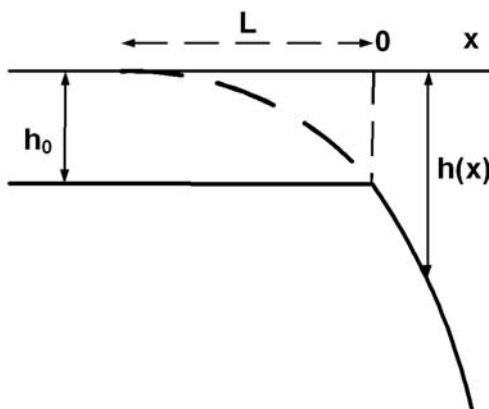
Figure 7. The geometry of a shallow coastal area and a convex slope.

depth ($x < 0$). Following the classical theory of long-wave reflection, the wavefield in this zone is presented by the superposition of the incident and reflected waves

$$\eta(x,t) = A_i \exp[i\omega(t - x/c_0)] + A_r \exp[i\omega(t + x/c_0)]. \quad (54)$$

Here $c_0 = \sqrt{gh_0}$ is the long-wave speed on an even bottom and A_i and A_r are the amplitudes of the incident and reflected waves, respectively. The monochromatic wave along the convex slope is described by equation (11). Assume that it has an amplitude A_0 at the point $x = 0$. At the inflection point the solutions expressed by equations (54) and (11) must match each other in terms of the continuity of the water level and the total discharge. These boundary conditions allow calculating the relative amplitudes of the reflected and transmitted waves from the following expressions for the coefficients of reflection and transmission:

$$\frac{A_r}{A_i} = -\frac{1}{1 + i\omega\tau}, \frac{A_0}{A_i} = \frac{i\omega\tau}{1 + i\omega\tau}, \quad (55)$$

where $\tau = 6L/c_0$. These amplitudes depend on ratio of the wave frequency (period) and the travel time of wave propagation to the zone of variable depth. As expected, for steep bottom slopes ($\omega\tau \ll 1$) the wave is almost completely reflected and experiences a phase shift of 180°. For gentle slopes ($\omega\tau \gg 1$) the incident wave passes to the zone of variable depth almost without reflection.

[48] Another important particular case is the reflection of a solitary wave propagating offshore. In this case equation (55) presents the operator form of the ordinary differential equation (that can be obtained from this equation by replacing $i\omega$ by d/dt)

$$\eta_r(t) + \tau\frac{d\eta_r}{dt} = -\eta_i(t). \quad (56)$$

This equation allows finding reflected waves in the vicinity of the inflection point if an incident wave at the same point is known. The details of the dispersion relation transformation to differential equations for the general case are

described by *Whitham* [1974]. The reflected wave can be calculated as an integral

$$\eta_r(t) = -\frac{\exp(-t/\tau)}{\tau} \int_0^t \eta_i(z) \exp(z/\tau)dz, \quad (57)$$

where it is assumed that the reflected wave is absent before the incident wave approaches the inflection point. If the incident wave is a pulse of finite duration T ($0 < t < T$) then from equation (57) it follows that the reflected wave amplitude at the inflection point exponentially decreases after passing the incident wave $t > T$

$$\eta_r(t > T) = -\frac{\exp(-t/\tau)}{\tau} \int_0^T \eta_i(z) \exp(z/\tau)dz. \quad (58)$$

Sometimes it is said that the reflected waves have an exponentially decreasing tail in such cases.

[49] From equation (58) it follows that the solitary wave in the water channel may entirely cross the convex slope and the inflection point without any loss of its energy. This happens for specific shapes of the incident wave and specific values of beach parameters, for which integral in equation (58) is zero. We do not include these cases in our analysis.

[50] From equation (56) it follows that

$$\int_{-\infty}^{+\infty} \eta_r(t)dt = -\int_{-\infty}^{+\infty} \eta_i(t)dt. \quad (59)$$

Thus, if the incident wave is a wave of elevation (pure crest), a wave of depression (pure trough) dominates in the reflected wave. This feature can be interpreted as a generalization of the property of the shape inversion in the process of reflection from the coastline as discussed above.

[51] As an example of the transformation of a wave pulse with a limited duration, we consider an incident sine pulse (Figure 8)

$$\eta_i(t) = A\begin{cases} \sin(\Omega t) & 0 < \Omega t < \pi \\ 0 & \text{out of the interval} \end{cases}. \quad (60)$$
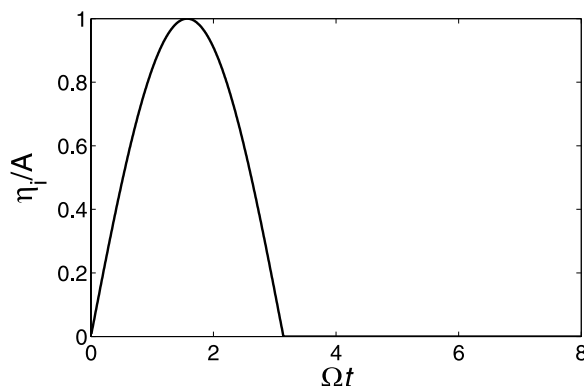
Figure 8. The relative water surface elevation in an incident wave described by equation (60).
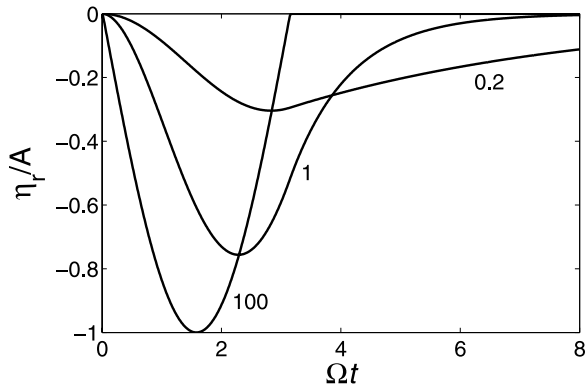
Figure 9. The shape of reflected waves for various values of parameter q.

An important feature of such a pulse is that it originally contains discontinuities of the surface slope that are gradually smoothed in the process of propagation. The profile of the surface elevation in the reflected wave, computed from equation (57), is

$$\eta_r(t) = -A\frac{q}{1+q^2}$$
$$\cdot \begin{cases} 0 & \Omega t < 0 \\ \exp(-q\Omega t) + q\sin(\Omega t) - \cos(\Omega t) & 0 < \Omega t < \pi, \\ (1 + \exp(q\pi))\exp(-q\Omega t) & \pi < \Omega t \end{cases}$$

$$(61)$$

where

$$q = \frac{1}{\Omega\tau} = \frac{\tan\theta}{8\Omega}\sqrt{\frac{g}{h}}, \qquad (62)$$

where θ is the angle at the inflexion point.

[52] In accordance with the above analysis, the shape of the reflected wave is inverted for all values of the parameter q (Figures 9 and 10). Its amplitude decreases and its tail becomes gradually longer. The growth of the tail is more pronounced for gentle beaches. The shape of the wave reflected from steep beaches is almost the same as for incident wave but has an opposite polarity.
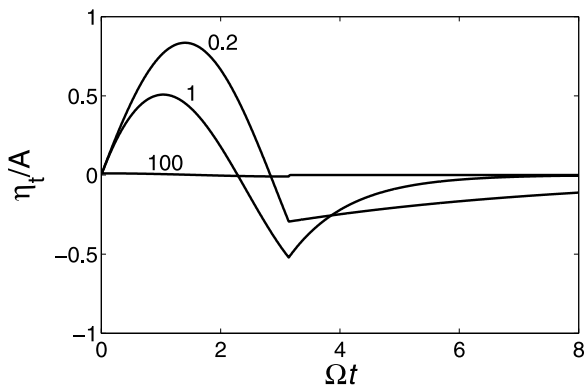
[53] Expressions (61) and (62) describe the shape of the reflected wave near the inflection point. It is straightforward to show, using Fourier superposition of the spectral components [equation (54)], that the reflected wave preserves its shape at all distances from the inflection point.

[54] The transmitted wave in the immediate region of the inflection point can be found from the boundary condition of continuity of water displacement

$$\eta_t(t) = \eta_i(t) + \eta_r(t). \qquad (63)$$

Because of equation (59), condition (16) is satisfied automatically, a feature that was expected for the traveling wave solution (see section 2) and confirmed here by equations (63) and (59).

[55] The oscillations of the water level in the immediate vicinity of the inflection point are of specific influence, because they can be the starting point of studies to further describe wave attack and runup with the use of more detailed models of the coastal zone. The time series of water surface at this point is presented in Figure 10 for the incident sine pulse. It demonstrates that a sign-variable wave is excited and propagates onshore after the inflection point. As expected, the amplitude of this wave is quite small in the case of steep convex beaches, yet almost full transmission may occur if the convex section of the beach has a moderate slope.

[56] According to equation (12), the transmitted wave does not change its shape in time, but its amplitude and phase do change with the distance from the inflection point. The shape of the velocity field in a transmitted wave changes with distance as well, see equation (15). In the immediate vicinity of the inflection point, the velocity of wave particles can be found from the continuity of discharge boundary condition

$$u_t(t) = \sqrt{\frac{g}{h_0}}[\eta_i(t) - \eta_r(t)]. \qquad (64)$$

Velocity time series are presented in Figure 11 for the case of an incident sine pulse for several values of parameter q. The velocity is always positive (as for incident wave). The velocity pulse is, however, somewhat modified and contains an elongated tail, the effective duration of which is longer

Figure 10. The shape of transmitted wave after the inflection point for various values of parameter q.
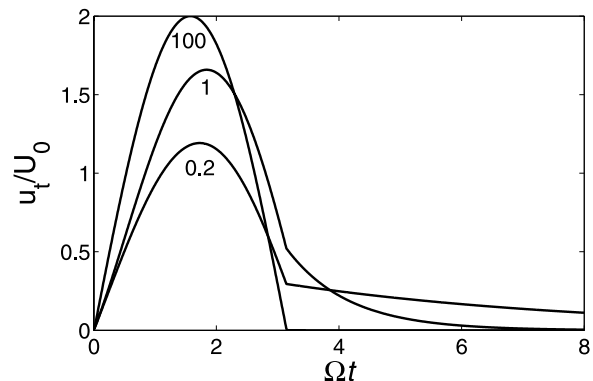
Figure 11. The shape of transmitted velocity after the inflection point for various values of parameter q.

for gently sloping beaches. The shape of the velocity variations in a transmitted wave varies with distance according to equation (15) and do not necessarily follow the shape of the water surface displacements. Nevertheless, far from the inflection point, the first term in equation (15) dominates and the shape of the velocity variations matches the shape of surface displacements. These processes are illustrated in Figure 11.

7. Conclusions and Discussion

[57] The above analysis of linear long-wave dynamics in a basin of variable depth confirms the intuitively obvious conjecture that simple, analytical traveling wave solutions of the variable coefficient wave equation (1) exist for a very limited number of situations. In fact, such solutions exist for a convex-shaped bottom, the water depth along which increases as $h(x) \sim x^{4/3}$. For this particular case a 1:1 transformation exists, which converts the general 1-D wave equation into an analogous equation with constant coefficients. In other words, the analyzed situation is the sole case in which the patterns of complex dynamics and reflections of long waves propagating over an uneven bottom can be fully described in terms of simple solutions for a basin of constant depth. Notice that another generic form of the wave equation allows such solutions for another profile ($h \sim x^4$) of the coastal slope and in this case the wave equation for velocity is solved [*Didenkulova et al.*, 2008].

[58] The obvious benefit of the existence of such solutions it that quite complex wave phenomena can be analyzed with the use of the large pool of results obtained for certain seabed shapes. This allows us to get important insight into how long traveling waves behave when approaching convex sections of the ocean coasts. While the majority of properties of wave propagation along a convex bottom mirrors those occurring in the basin of linearly varying depth, some interesting distinguishing features become evident; for example, the shapes of water displacement and velocity in the traveling wave do not coincide. As expected, the general solution of the Cauchy problem to the wave equation for water displacement in the case of the convex bottom profile in question is expressed through two traveling waves propagating in opposite directions. It is demonstrated that the wave amplitude satisfies the Green's law even for not smoothly varied bottom. The situation is more complicated in the case of water velocity, where a zone of space-variable currents generally exists between these two waves. Such a zone cannot be presented by the sum of two pure traveling waves and inevitably contains certain other motion components. As the additional components cannot be generated out of interaction of these two linear waves, they must be born through a specific reflection and transition processes. That is why we use inverted commas when speaking about a nonreflecting beach.

[59] More generally, the convex beach in question possesses somewhat unexpectedly strong reflective features. Additionally to producing the above discussed local current, the boundary condition for the flow at the shoreline ($H = 0$) produces the result equivalent to the one occurring if there were a vertical wall at the coastline. This feature may lead to

prominent energy reflection from certain realistic coasts with very shallow coastal areas.

[60] A very interesting feature is that runup of certain wave classes on a beach with this sort of bottom relief may be considerably higher than for a beach with a linear profile, and with an equal mean slope. This property has been shown to hold for shallow water Korteweg-de Vries solitary waves (solitons) which frequently are used as a convenient model of tsunami waves. It is also shown that the shape of the water oscillations at the shoreline is determined by the first derivative of the incident waveshape. As a result, if the incident wave has a steep front, the runup height will be higher. This property is in line with recent developments in the theory of runup of asymmetric waves that indicate a strong dependence of the runup height for waves of equal height on the steepness of the face slope of the wave [*Didenkulova et al.*, 2006, 2007].

[61] Although initial development of the pair of waves from a wave of elevation (or depression) may lead to the formation of two waves of elevation (depression), a sign-variable shape of the whole wavefield is necessarily created after some time. Similarly, if the incident wave approaches a zone of increasing depth, the reflected onshore-going wave has a sign-variable shape. This reflection inverts the sign of the surface disturbance and creates a wavefield consisting of both elevations and depressions for any initial waveshape.

[62] This particular, rigorous result of our analysis has no simple interpretation in practical applications. The inversion of the sign of the water surface elevation is a principally new feature of this geometry which does not become evident in the theory of wave reflection from a plane slope or a vertical wall. Notice that it results neither from the presence of a singularity of the beach at the shoreline $x = 0$ (in the sense that the bottom profile touches the water surface at the shoreline) nor from an imperfect choice of the boundary conditions. Instead, this phenomenon becomes apparent because of specific properties of wave reflection from convex profiles, during which phase shifts larger than $\pi/2$ may occur. This property serves as one of the fundamental differences of the reflections under discussion from those that occur at concave beaches (including from those having the shape of the Dean's Equilibrium Profile) and that have phase shifts in the range from 0 to $\pi/2$.

[63] Although the exact results of the above studies are valid for a limited class of bottom profiles, they are eventually approximately correct for a much wider class of basins with a convex bottom slope, or containing extensive sections of such slopes. An important aspect to be mentioned once more is that the performed analysis does not require slow variation of the basin depth and remains valid for quite large slopes. This property opens perspectives for extensive use of the obtained solutions and results for developing practically usable models of, for example, tsunami waves, and also provides new perspectives in the development of the weakly nonlinear theory of water waves in a basin of variable depth.

References

Babich, V. M., and V. S. Buldyrev (1991), *Short-Wavelength Diffraction Theory: Asymptotic Methods*, 456 pp., Springer, Berlin.

Berry, M. V. (2005), Tsunami asymptotics, *New J. Phys.*, 7, 129–147.

Brekhovskikh, L. M. (1980), *Waves in Layered Media*, 343 pp., Academic, New York.

Carrier, G. F., and H. P. Greenspan (1958), Water waves of finite amplitude on a sloping beach, *J. Fluid Mech.*, 4, 97–109, doi:10.1017/S0022112058000331.

Carrier, G. F., T. T. Wu, and H. Yeh (2003), Tsunami run-up and draw-down on a plane beach, *J. Fluid Mech.*, 475, 79–99, doi:10.1017/S0022112002002653.

Cherkesov, L. V. (1976), *Hydrodynamics of Surface and Internal Waves* (in Russian), 364 pp., Naukova Dumka, Kiev.

Dalrymple, R. A., S. T. Grilli, and J. T. Kirby (2006), Tsunamis and challenges for accurate modelling, *Oceanography*, 19(1), 142–151.

Dean, R. G., and R. A. Dalrymple (2002), *Coastal processes With Engineering Applications*, 475 pp., Cambridge Univ. Press, Cambridge, U. K.

Didenkulova, I. I., and E. N. Pelinovsky (2008), Run-up of long waves on a beach: The influence of the incident wave form, *Oceanology*, 48, 1–6, doi:10.1007/s11491-008-1001-y.

Didenkulova, I. I., N. Zahibo, A. A. Kurkin, B. V. Levin, E. N. Pelinovsky, and T. Soomere (2006), Runup of nonlinearly deformed waves on a coast, *Dokl. Earth Sci.*, 411, 1241–1243, doi:10.1134/S1028334X06080186.

Didenkulova, I., E. Pelinovsky, T. Soomere, and N. Zahibo (2007), Runup of nonlinear asymmetric waves on a plane beach, in *Tsunami and Nonlinear Waves*, edited by A. Kundu, pp. 173–188, Springer, Berlin.

Didenkulova, I. I., E. N. Pelinovsky, and T. Soomere (2008), Exact travelling wave solutions in strongly inhomogeneous media, *Estonian J. Eng.*, 57(3), 220–231, doi:10.3176/eng.2008.3.03.

Dingemans, M. W. (1996), *Water Wave Propagation Over Uneven Bottom*, World Sci., Singapore.

Dobrokhotov, S. Y., S. A. Sekerzh-Zenkovich, B. Tirozzi, and B. Volkov (2006), Explicit asymptotics for tsunami waves in framework of the piston model, *Russ. J. Earth Sci.*, 8, ES4003, doi:10.2205/2006ES000215.

Dobrokhotov, S. Y., S. O. Sinitsyn, and B. Tirozzi (2007), Asymptotics of localized solutions of the one-dimensional wave equation with variable velocity. Part 1. The Cauchy problem, *Russ. J. Math. Phys.*, 14, 28–56, doi:10.1134/S1061920807010037.

Dutykh, D., F. Dias, and Y. Kervella (2006), Linear theory of wave generation by a moving bottom, *C. R. Math.*, 343, 499–504.

Ginzburg, V. L. (1970), *Propagation of Electromagnetic Waves in Plasma*, 683 pp., Pergamon, New York.

Grimshaw, R. (1970), The solitary waves in water of variable depth, *J. Fluid Mech.*, 42, 639–656, doi:10.1017/S0022112070001520.

Gusiakov, V. M. (2002), Historical Tsunami Database, http://www.ngdc.noaa.gov/hazard/tsu_db.shtml, Natl. Geophys. Data Cent., Novosibirsk, Russia.

Kaistrenko, V. M., R. K. Mazova, E. N. Pelinovsky, and K. V. Simonov (1991), Analytical theory for tsunami run up on a smooth slope, *Int. J. Tsunami Soc.*, 9, 115–127.

Kânoğlu, U. (2004), Nonlinear evolution and runup-drawdown of long waves over a sloping beach, *J. Fluid Mech.*, 513, 363–372, doi:10.1017/S002211200400970X.

Kânoğlu, U., and C. Synolakis (2006), Initial value problem solution of nonlinear shallow water-wave equations, *Phys. Rev. Lett.*, 97, 148501.1–148501.4, doi:10.1103/PhysRevLett.97.148501.

Kit, E., and E. Pelinovsky (1998), Dynamical models for cross-shore transport and equilibrium bottom profiles, *J. Waterw. Port Coastal Ocean Eng.*, 124(3), 138–146, doi:10.1061/(ASCE)0733-950X(1998)124:3(138).

Kobayashi, N. (1987), Analytical solution for dune erosion by storms, *J. Waterw. Port Coastal Ocean Eng.*, 113(4), 401–418, doi:10.1061/(ASCE)0733-950X(1987)113:4(401).

Le Blond, P. H., and L. A. Mysak (1978), *Waves in the Ocean*, Elsevier, Amsterdam.

Madsen, P. A., and D. R. Fuhrman (2007), Run-up of tsunamis and long waves in terms of surf-similarity, *Coastal Eng.*, 55, 209–223, doi:10.1.0165coastaleng2007.09.007.

Maslov, V. P. (1987), *Asymptotic Methods for Solving Pseudo-Differential Equations* (in Russian), Nauka, Moscow.

Maslov, V. P. (1994), *The Complex WKB Method for Nonlinear Equations 1: Linear Theory*, 300 pp., Birkhauser, Basel, Germany.

Massel, S. R. (1989), *Hydrodynamics of Coastal Zones*, 336 pp., Elsevier, Amsterdam.

Mazova, R. K., N. N. Osipenko, and E. N. Pelinovsky (1991), Solitary wave climbing a beach without breaking, *Rozprawy Hydrotech.*, 54, 71–80.

Mei, C. C. (1989), *The Applied Dynamics of Ocean Surface Waves*, 740 pp., World Sci., Singapore.

Ostrovsky, L. A., and E. N. Pelinovsky (1970), Wave transformation of the surface of a fluid of variable depth, *Izv. Russ. Acad. Sci. Atmos. Oceanic Phys., Engl. Transl.*, 6, 552–555.

Pedersen, G., and B. Gjevik (1983), Runup of solitary waves, *J. Fluid Mech.*, 135, 283–299, doi:10.1017/S0022112083003080.

Pelinovsky, E. (1996), *Hydrodynamics of Tsunami Waves* (in Russian), 276 pp., Appl. Phys. Inst., Nizhny Novgorod, Russia.

Pelinovsky, E., and R. Mazova (1992), Exact analytical solutions of nonlinear problems of tsunami wave run-up on slopes with different profiles, *Nat. Hazards*, 6, 227–249, doi:10.1007/BF00129510.

Shen, M. C. (1975), Ray method for surface waves on fluid of variable depth, *SIAM Rev.*, 17, 38–56, doi:10.1137/1017003.

Soomere, T., A. Kask, J. Kask, and R. Nerman (2007), Transport and distribution of bottom sediments at Pirita Beach, *Estonian J. Earth Sci.*, 56(4), 233–254.

Sretensky, L. N. (1977), *Theory of Wave Motions in Fluids* (in Russian), 816 pp., Nauka, Moscow.

Steetzel, H. J. (1993), *Cross-Shore Transport During Storm Surges*, Delft Hydr., Delft, Netherlands.

Stoker, J. (1957), *Water Waves*, Wiley, New York.

Synolakis, C. E. (1987), The runup of solitary waves, *J. Fluid Mech.*, 185, 523–545, doi:10.1017/S002211208700329X.

Synolakis, C. E. (1991), Tsunami runup on steep slopes: How good linear theory really is?, *Nat. Hazards*, 4, 221–234, doi:10.1007/BF00162789.

Tadepalli, S., and C. E. Synolakis (1994), The runup of N waves, *Proc. R. Soc. London Ser. A*, 445, 99–112, doi:10.1098/rspa.1994.0050.

Tinti, S., and R. Tonini (2005), Analytical evolution of tsunamis induced by near-shore earthquakes on a constant-slope ocean, *J. Fluid Mech.*, 535, 33–64, doi:10.1017/S0022112005004532.

Tinti, S., E. Bortolucci, and C. Chiavettieri (2001), Tsunami excitation by submarine slides in shallow-water approximation, *Pure Appl. Geophys.*, 158, 759–797, doi:10.1007/PL00001203.

Whitham, G. B. (1974), *Linear and Nonlinear Waves*, 636 pp., Wiley, New York.

————————————
I. Didenkulova and T. Soomere, Institute of Cybernetics, Tallinn University of Technology, Akadeemia Tee 21, 12618 Tallinn, Estonia. (ira@cs.ioc.ee)

E. Pelinovsky, Department of Nonlinear Geophysical Processes, Institute of Applied Physics, Russian Academy of Sciences, 46 Uljanov Street, Nizhny Novgorod, 603950 Russia.